Int. J. Dynam. Control
DOI 10.1007/s40435-015-0184-z

TADC: a new three-axis detumbling mode control approach

A. H. Mazinan[1] · A. R. Khalaji[2]

Received: 15 March 2015 / Revised: 10 May 2015 / Accepted: 25 May 2015

Abstract A new three-axis detumbling mode control approach, namely TADC in the present research, is investigated to deal with a spacecraft, in a short period of time. In a word, the study considers the problem of detumbling by means of system modelling, while the proposed control approach in agreement with the simulation results can be of novelty with respect to the other related potential benchmarks. The approach proposed here plays an important role in this area to adjust angular velocities in the three axes regarding the system under control to be desirable. In some cases, to guarantee the system stability in the process of missions, the whole of angular velocities are to be accurate. In fact, it aims us to organize a number of programmed maneuvers including the orbital, the thermal and so on to be efficient. The idea behind the approach is organized in line with a linear control approach, since the pulse-width pulse-frequency modulator is employed in association with the control allocation to cope with a set of on–off thrusters. Hereinafter, the number of these on–off thrusters may be increased with respect to the investigated control laws to provide overall accurate performance of the spacecraft through the control allocation. The effectiveness of the approach investigated here is finally considered by organizing four scenarios of the experiments and also comparing the outcomes with a number of potential benchmarks.

Keywords Detumbling mode control approach · Three-axis angular velocities · Control allocation · Spacecraft dynamics · On–off thrusters · Pulse-width pulse-frequency modulator

1 Introduction

A number of efficient and applicable studies on the spacecraft attitude control have been carried out during the past decades. One of main issues regarding the present complex and complicated system is to deal with the angular velocities in the three axes, in order to prepare the process of missions, appropriately. In fact, a number of programmed maneuvers including the orbital, the thermal and so on can be organized, provided that these angular velocities are adjusted to be desirable. As an example, in the spaceflight, the orbital maneuver is known as the use of propulsion systems, in order to change the orbit of the spacecraft from initial to its final one, in a very careful manner. Due to the fact that this control item plays an important role to guarantee the stability of the system, state-of-the-art in this area is always appreciated by related experts. It is obvious that the number of potential materials in the field of detumbling mode control is truly rare and therefore some new insights are certainly appropriate to investigate. With this purpose, the idea of the control approach, which is proposed here, has to first be developed through pulse-width pulse-frequency (PWPF) modulator, which is able to handle a set of on–off thrusters. Furthermore, the number of these on–off thrusters could be increased in line with the investigated control efforts to provide overall accurate performance

✉ A. H. Mazinan
ahmazian@gmail.com; mazinan@azad.ac.ir; ah_mazinan@yahoo.com

1 Department of Control Engineering, Faculty of Electrical Engineering, South Tehran Branch, Islamic Azad University (IAU), No. 209, North Iranshahr St., P.O. Box 11365/4435, Tehran, Iran

2 Department of Control Engineering, Student of Electrical Engineering, South Tehran Branch, Islamic Azad University (IAU), No. 209, North Iranshahr St., P.O. Box 11365/4435, Tehran, Iran

Published online: 03 June 2015

regarding the spacecraft, as long as the control allocation (CA) is correspondingly realized.

1.1 Related works

Concerning the recent potential investigations in this area, many attentions have been paid on the detumbling of a rigid spacecraft via torque wheel in association with gyroscopic motion [1], where the angular motion of a satellite, which is equipped with the active magnetic attitude control system, is introduced [2]. Attitude stabilization of the satellite through an optimal control strategy is presented [3], while the vehicle system dynamics is reviewed for the purpose of developmenting high-speed trains [4]. In making another effort, the generalized projective synchronization of chaotic satellites is suggested through linear matrix inequality [5], where a method of delay compensation in the area of attitude control of flexible spacecraft is presented [6]. The useful practical information regarding the spacecraft dynamics and its control is investigated [7], where the modeling and the corresponding simulation regarding the aerospace vehicle dynamics is suggested [8]. Autonomous attitude coordinated control is proposed for the spacecraft [9], since nonlinear attitude tracking control is suggested for the same spacecraft [10]. Finite-time fault tolerant attitude stabilization control is made as another research in the area of rigid spacecraft [11].

Hereinafter, an attitude synchronization control is considered for a class of flexible spacecrafts to deal with the problem of attitude synchronization [12]. Another research work is to realize finite-time control for nonlinear spacecraft attitude via terminal sliding mode approach [13]. Other insight in this field is to deal with an adaptive attitude tracking control for the rigid spacecraft with finite-time convergence [14]. Review of the spacecraft attitude determination and its control is completed using the quaternion based method [15]. An adaptive fuzzy fault-tolerant attitude control is considered for the spacecraft [16]. The other idea is to realize robust attitude control for the spacecraft under assigned velocity and control constraints [17], while consideration for the leader-following attitude control of the multiple rigid spacecrafts is completed [18]. Furthermore, the attitude dynamics of the miniature spacecraft and the corresponding control are considered via pseudo-wheels [19], once the attitude control for the rigid spacecraft is investigated with the disturbances that are generated by time varying exo-systems [20].

Robust decentralized attitude coordination control of the spacecraft formation is considered [21], where the outcomes in robust fault-tolerant tracking control are presented for the spacecraft under control input saturation [22]. A control approach is designed for the attitude tracking of the rigid spacecraft with actuator saturation [23], once an optimal sliding mode control approach is suggested in the attitude tracking for the spacecraft via Lyapunov function [24]. Afterwards, time-varying sliding mode controls in the area of rigid spacecraft attitude tracking are presented [25], while adaptive sliding mode control with its application to six-DOF relative motion of the spacecraft under input constraint is given, as another outcome, in this field [26]. Furthermore, adaptive backstepping fault-tolerant control is implemented for the flexible spacecraft under unknown bounded disturbances as well as actuator failures and the realization of the attitude control for the spacecraft is illustrated [27]. Another research is to realize finite-time coordinated tracking control of the spacecraft formation that is considered without velocity measurements [29].

Regarding the PWPF research, there are various literatures in this area, where one of the best is to describe the optimal tuning of the PWPF modulator in the area of the attitude control, in a constructive manner [30]. Regarding the CA research, the subject suggests the advantage of a modular design, as long as the high-level motion control algorithm is designed. There is no detailed knowledge about the effectors and actuators. The objective of the research is to survey the CA approaches, which are motivated by the wide range of applications that have expanded in the aerospace and maritime industries [31]. Dynamic allocation for input redundant control systems is made as another effort. It is proposed to address control systems under redundant actuators [32], where the relevant research is to deal with the CA for gimbaled/fixed thrusters [33].

As are obvious, the whole of the above-referenced research in association with other related potential works are all tried to address some efficient methods to deal with this complicated system. In the same way, the proposed TADC has now made as another new effort, while its main differences with respect to these methods are given in the approach's structure and the corresponding results.

The rest of the manuscript is organized as follows: The proposed TADC approach including 'the spacecraft dynamics', 'the PWPF modulator realization' and 'the CA scheme realization' are first given in Sect. 2. The simulation results are then given in Sect. 4. Finally, the research concludes the investigated outcomes in Sect. 5.

2 The proposed TADC approach

The schematic diagram of the proposed TADC approach is now illustrated in Fig. 1. The control method is organized based upon a closed loop system including the proportional derivative (PD), the PWPF modulator, the CA and finally the spacecraft dynamics by tracking the angular velocity commands at each instant of time $(AV_{com}(t))$. The responsibility of the present PD is to deal with the three-axis angular velocities of the spacecraft to guarantee the tracking performance,

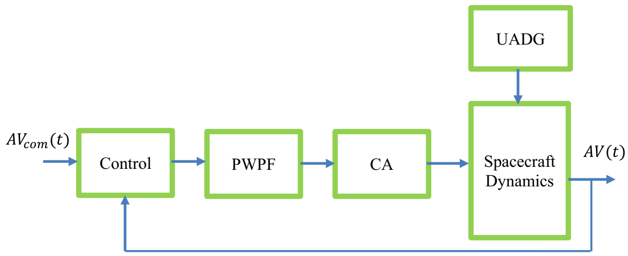

Fig. 1 The schematic diagram of the proposed TADC approach

in an accurate manner, instantly. In the same way, the PWPF modulator is realized in association with the CA to produce the appropriate control efforts, at each instant of time, to handle the spacecraft. It should be noted that the widths and also the frequencies of the pulses, generated through the PWPF modulator, are accurately adjusted in the three axes, in order to maintain the best control efforts for the spacecraft. Due to the fact that the number of on–off thrusters is not usually taken as the three-axis control efforts, the CA needs to be employed. In fact, the signals, produced through the CA, are applied to these on–off thrusters. Meanwhile, the rest of the modules, employed in the proposed approach, are listed as the three-axis desired referenced generator module, the data conversion module, the inverse data conversion module and finally the uncertainties and disturbances generator (UADG).

Regarding the three-axis desired referenced generator module, it is realized to produce the desired angular velocities in the three axes in degree per second, while they have to be tracked though the proposed TADC approach, carefully. It should be noted that the procedure of controlling regarding the approach presented here is to deal with the whole of angular velocities in radian per second. In this way, the duty of the data conversion module is to convert degree per second to radian per second, while the duty of the corresponding data conversion module is to convert radian per second to degree per second, as well. Some of these subsystems, for simplicity, are avoided presenting in the following schematic diagram.

3 The spacecraft dynamics

An acceptable assumption allows us to pursue the attitude dynamics that is independent of the translational motion. According to the Newton's second law, the summation of the external moments in the body frame, i.e. 'B' can be equal to the time rate of the angular momentum variations, in the inertial frame ($D^I\left(h_B^{BI}\right) = m_B$). In the same way, transferring the rotational time in the body frame can be written as [7,8]

$$D^I\left(I_B^B\omega^{BI}\right) + \Omega^{BI} I_B^B \omega^{BI} = \sum m_B \tag{1}$$

where I_B^B is taken as spacecraft's moments of inertia, ω^{BI} is taken as spacecraft's angular rates, relative to the inertial coordinate system and $\Omega^{BI}$is taken as its skew symmetric matrix. Picking body coordinate $]^B$, the closed-form equations can be acquired by the following

$$\left[I_B^B\right]^B \left[\frac{d\omega^{BI}}{dt}\right]^B + \left[\Omega^{BI}\right]^B \left[I_B^B\right]^B \left[\omega^{BI}\right]^B = \left[\sum m_B\right]^B \tag{2}$$

Now, $p = w_x, q = w_y, r = w_z$ are assumed as spacecraft's angular velocities in the three axes, φ, θ, ψ are taken as the Euler angles and also $\tau_i, I_{ii}; j = x, y, z$ are taken as the control torques and the moments of inertia, respectively, in the same axes. The nonlinear model of the spacecraft is resulted by the following

$$\begin{cases} \dot{p} = \frac{\tau_x}{I_{xx}} - \frac{(I_{zz}-I_{yy})}{I_{xx}} qr \\ \dot{q} = \frac{\tau_y}{I_{yy}} - \frac{(I_{xx}-I_{zz})}{I_{yy}} pr \\ \dot{r} = \frac{\tau_z}{I_{zz}} - \frac{(I_{yy}-I_{xx})}{I_{zz}} pq \\ \dot{\varphi} = p + (\tan\theta \sin\varphi) q + (\tan\theta \cos\varphi) \\ \dot{\theta} = (\cos\varphi) q - (\sin\varphi) r \\ \dot{\psi} = \left(\frac{\sin\varphi}{\cos\theta}\right) q + \left(\frac{\cos\varphi}{\cos\theta}\right) r \end{cases} \tag{3}$$

where

$$\begin{cases} I_{xx} = \int_m (y^2 + z^2) dm \\ I_{yy} = \int_m (x^2 + z^2) dm \\ I_{zz} = \int_m (x^2 + y^2) dm \end{cases} \tag{4}$$

In the sequel, to deal with the linear model of the spacecraft in the form of $\dot{X} = AX + BU$, the state vector including $X = \left[\, p \; q \; r \; \phi \; \theta \; \varphi \,\right]^T$ and the control efforts including $U = \left[\tau_x \; \tau_y \; \tau_z \; 0 \; 0 \; 0\right]^T$ are taken. Now, the linear model of the spacecraft is correspondingly resulted by

$$A=\begin{bmatrix} 0 & \frac{-r_0 I_{zz}+r_0 I_{yy}}{I_{xx}} & \frac{-q_0 I_{zz}+q_0 I_{yy}}{I_{xx}} & 0 & 0 & 0 \\ \frac{-r_0 I_{zz}+r_0 I_{yy}}{I_{xx}} & 0 & \frac{-p_0 I_{xx}+p_0 I_{zz}}{I_{yy}} & 0 & 0 & 0 \\ \frac{-r_0 I_{zz}+r_0 I_{yy}}{I_{xx}} & \frac{-p_0 I_{xx}+p_0 I_{zz}}{I_{yy}} & 0 & 0 & 0 & 0 \\ 1 & \sin\varphi_0\tan\theta_0 & \cos\varphi_0\tan\theta_0 & q_0\cos\varphi_0\tan\theta_0-r_0\sin\varphi_0\tan\theta_0 & \frac{r_0\cos\varphi_0+q_0\sin\varphi_0}{\cos^2\theta_0} & 0 \\ 0 & \cos\varphi_0 & -\sin\varphi_0 & -q_0\sin\varphi_0-r_0\cos\varphi_0 & 0 & 0 \\ 0 & \frac{\sin\varphi_0}{\cos\theta_0} & \frac{\cos\varphi_0}{\cos\theta_0} & \frac{q_0\cos\varphi_0-r_0\sin\varphi_0}{\cos\theta_0} & \frac{q_0\sin\varphi_0\sin\theta_0+r_0\cos\varphi_0\sin\theta_0}{\cos^2\theta_0} & 0 \end{bmatrix} \tag{5}$$

and the following

$$B=\begin{bmatrix} \frac{1}{I_{xx}} & 0 & 0 & 0 & 0 & 0 \\ 0 & \frac{1}{I_{yy}} & 0 & 0 & 0 & 0 \\ 0 & 0 & \frac{1}{I_{zz}} & 0 & 0 & 0 \\ 0 & 0 & 0 & 0 & 0 & 0 \\ 0 & 0 & 0 & 0 & 0 & 0 \\ 0 & 0 & 0 & 0 & 0 & 0 \end{bmatrix} \tag{6}$$

where the initial state vector is taken as $X_0 = [p_0\ q_0\ r_0\ \phi_0\ \theta_0\ \varphi_0]^T$ and the operating point of the system is taken as $p = q = r = \varphi = \psi = 0$.

3.1 The PWPF modulator realization

The PWPF modulator can be used in so many environments such as the spacecrafts. The various modulation methods have been realized to consider the level of the required torque, the width and the frequency of pulses, due to the fact that the reaction control approaches do not possess the linear relationship between the input to the controller and its output torque. To shape the nonlinear output of on–off thrusters into the linear output, a number of thruster control techniques are to be exploited. It can be shown that the PWPF modulator is employed in the various applications, frequently. Others like the Schmitt trigger control, the pseudo rate modulator, the integrated pulse frequency modulator and the pulse width modulator are also considered, in order to shape the output of the thrusters. The PWPF modulator is now realized due to its advantages over other types of modulators. It is shown in Fig. 2 that the PWPF modulator is organized based upon the first order lag filter along with the Schmitt trigger through the closed loop system.

The PWPF modulator's parameters that are shown in the present schematic diagram need to be considered. In this regard, the static characteristics parameters are now tabulated in Table 1. The whole of parameters are needed to consider in the process of designing the modulator, accurately.

In order to present the applicability of the PWPF modulator, in a clear form, Fig. 3 is now illustrated [7,30].

It is easily obvious that by applying the constant value to the PWPF modulator, at each instant of time, the input and its output regarding the filter $\frac{K}{1+\tau s}$ are varied, where the final output regarding the PWPF modulator may be produced as a sequence of on–off pulses.

In general, some parameters of the PWPF modulator are initialized and tabulated in Table 2.

3.2 The CA scheme realization

The realization of the CA scheme is to command on distribution logic for selecting the specific thrusters and calculating their firing durations, in order to realize the force and the torque commands, which are derived from the control of the spacecraft. This scheme is briefly given as [31–33].

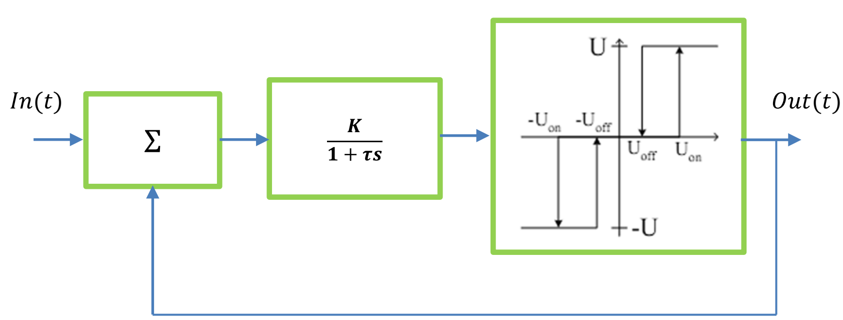

Fig. 2 The schematic diagram of the PWPF

Table 1 The static parameters of the PWPF modulator and its formula

	The parameter's description	The parameter's formula
1	On time	$t_{on} = -\tau Ln\left(1 - \frac{U_{on}-U_{off}}{K-KIn+U_{on}}\right) \approx \tau \frac{U_{on}-U_{off}}{K-KIn+U_{on}}; e^{\frac{-t_{on}}{\tau}} \approx 1 - \frac{t_{on}}{\tau}$
2	Off time	$t_{off} = -\tau Ln\left(1 - \frac{U_{on}-U_{off}}{KIn-U_{off}}\right) \approx \frac{U_{on}-U_{off}}{KIn-U_{off}}; e^{\frac{-t_{off}}{\tau}} \approx 1 - \frac{t_{off}}{\tau}$
3	Modulator frequency	$f = \frac{1}{t_{on}+t_{off}}$
4	Duty cycle	$DC = f.t_{on} = \frac{t_{on}}{t_{on}+t_{off}}$
5	Minimum input	$In_{min} = \frac{U_{on}}{K}$
6	Maximum input	$In_{max} = \frac{U_{off}}{K+1}$
7	BW	$\Delta = -\tau Ln\left(1 - \frac{h}{K}\right) \approx \frac{h\tau_m}{K}$

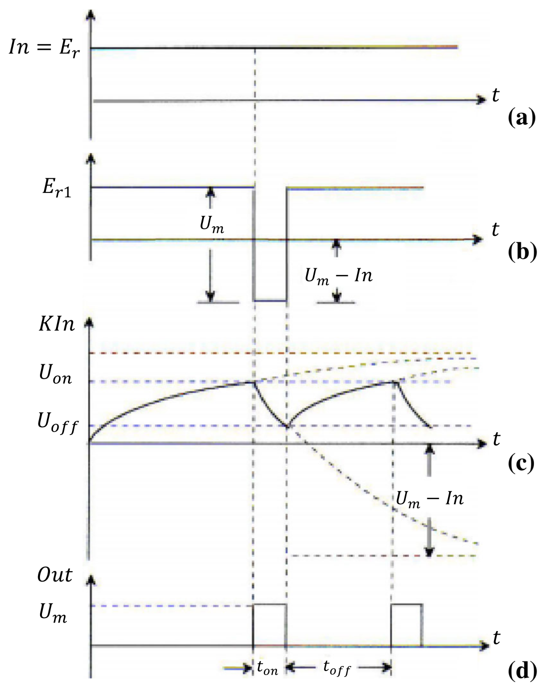

Fig. 3 **a** Constant value to the PWPF modulator, **b** the input of the filter $\frac{K}{1+\tau s}$, **c** the output of the filter $\frac{K}{1+\tau s}$, **d** the output of the PWPF modulator [7]

$$v(t) = Bu(t) \tag{7}$$

where $u(t)$ is taken as the real control and $v(t)$ is also taken as its virtual control, since B is taken as the constant matrix. The advantage of the CA scheme is to deal with a number of actuators, separately and efficiently. In order to realize the CA scheme, a pseudo inverse matrix needs to be calculated. With this purpose, the torque in the three axes including τ_x, τ_y and τ_z and the corresponding thruster's levels including $\delta_i; i = 1, 2, \ldots, n$ are presented by the following

Table 2 The PWPF modulator's parameters variations recommendation

	The parameters	The variations
1	K	2.5 : 7.5
2	τ	0.1 : 1.0
3	U_{on}	0.1 : 1.0
4	$h = U_{on} - U_{off}$	0.2 : $2U_{on}$

$$\begin{bmatrix} \tau_x \\ \tau_y \\ \tau_z \end{bmatrix} = E \begin{bmatrix} \delta_1 \\ \delta_2 \\ \vdots \\ \delta_n \end{bmatrix} \tag{8}$$

or

$$\begin{bmatrix} \delta_1 \\ \delta_2 \\ \vdots \\ \delta_n \end{bmatrix} = E^+ \begin{bmatrix} \tau_x \\ \tau_y \\ \tau_z \end{bmatrix} \tag{9}$$

By supposing the number of thrusters to be eight in the present research, the matrix in Eq. (10) could be resulted. It should be noted that the required number of thrusters, which are related to its physical configuration must appropriately be chosen to guarantee the desirable performance. It means that a penalty of budget may be created in the process of realizing the spacecraft, if the number of employed thrusters is incoherently increased. Meanwhile, a penalty may be created in the system performance, if the number of them is inappropriately decreased. Regarding the outcomes investigated here, the best choice is now finalized as

$$E = \begin{bmatrix} 0 & 0 & 0 & 0 & -R & -R & R & R \\ -R & 0 & R & 0 & 0 & L & 0 & -L \\ 0 & R & 0 & -R & L & 0 & -L & 0 \end{bmatrix} \tag{10}$$

And its pseudo-inverse is easily acquired by

$$E^{+}=\begin{bmatrix} 0 & \frac{-R}{2(L^2+R^2)} & 0 \\ 0 & 0 & \frac{R}{2(L^2+R^2)} \\ 0 & \frac{-R}{2(L^2+R^2)} & 0 \\ 0 & 0 & \frac{-R}{2(L^2+R^2)} \\ \frac{-1}{4R} & 0 & \frac{L}{2(L^2+R^2)} \\ \frac{-1}{4R} & \frac{L}{2(L^2+R^2)} & 0 \\ \frac{-1}{4R} & 0 & \frac{L}{2(L^2+R^2)} \\ \frac{-1}{4R} & \frac{L}{2(L^2+R^2)} & 0 \end{bmatrix} \tag{11}$$

Here, R and L are taken as thruster's arm and its length, respectively. The present constant parameters are highly variable with respect to the configuration of the thrusters in the spacecraft. It means that the results in the area of the CA scheme are directly based on the physical positions of the thrusters. In such a case, the relation between E and E^{+} can easily be presented through $E^{+}=E^{T}\left(EE^{T}\right)^{-1}$, as well . Now, by assuming $T_i; i=1,2,\ldots,8$ as thruster's level (N), the three-axis thrusts could clearly be calculated as

$$\begin{cases} \tau_x=-R\left(T_5+T_6-T_7-T_8\right) \\ \tau_y=R\left(T_3-T_1\right)+L\left(T_6-T_8\right) \\ \tau_z=R\left(T_2-T_4\right)+L\left(T_5-T_7\right) \end{cases} \tag{12}$$

Due to the fact that $\delta_i; i=1,2,\ldots,n$ in Eq. (9) have to be given in the amplitude of 0 and 1, the on–off relay with the notation of $f_{on/off}$ could be realized. In one such case, the generation of the present binary sequenced signals for the whole of on–off thrusters are truly guaranteed. Although, the control torques τ_x, τ_y and τ_z may be changed to its efficient control torques through τ_{x_e}, τ_{y_e} and τ_{z_e} by

$$\begin{bmatrix}\tau_{x_e}\\ \tau_{y_e}\\ \tau_{z_e}\end{bmatrix}=Ef_{on/off}\left(E^{+}\begin{bmatrix}\tau_x\\ \tau_y\\ \tau_z\end{bmatrix}\right) \tag{13}$$

It should be noted that the hysteresis; ε, of the $f_{on/off}$ relay may be optimized to present the efficient control torques.

4 The simulation results

The simulation results are carried out in line with the schematic diagram of the proposed TADC approach, illustrated in Fig. 1. The spacecraft that is now under control is known as an applicable system with the key specifications, tabulated in Table 3. These parameters are calculated or initiated in the process of realizing the proposed control approach.

The tracking performance of the proposed control approach is first considered by evaluating the angular velocities of the spacecraft in the three axes, i.e. x, y, z. Moreover, the set of thruster's commands are then considered, in the four scenarios of the experiments. Regarding the first one, Fig. 4 illustrates the results of the system by applying the desired commands including 0.03, 0.03, 0.04 °/s to the approach.

Table 3 The parameters used in the proposed approach

	The values	The parameters
1	$\begin{cases} I_x=20 \\ I_y=100 \\ I_z=100 \end{cases}$	Moments of inertia
2	$T=5.0$	Thruster's level
3	$\begin{cases} k_{px}=5.0 \\ k_{py}=5.0 \\ k_{pz}=5.0 \end{cases}$	Control coefficients
4	$\begin{cases} k_m=5.0 \\ T_m=0.8 \\ U_{on}=0.8 \\ U_{off}=0.1 \end{cases}$	Three-axis PWPF coefficients
5	$\begin{cases} L=0.20 \\ R=0.40 \end{cases}$	Thruster's configuration

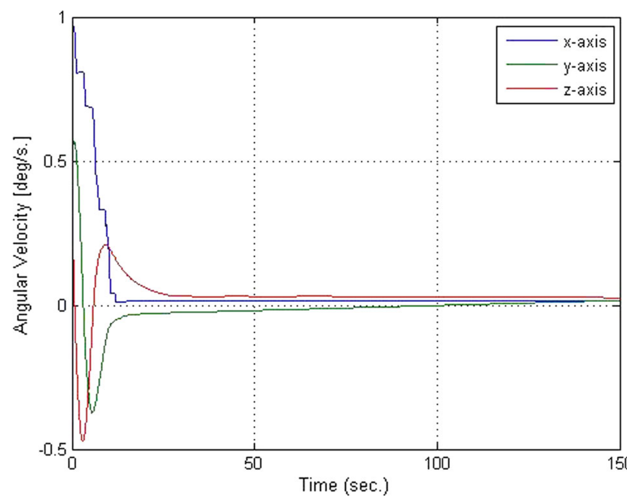

Fig. 4 The tracking of three-axis angular velocities of the system in the 1st experiment

Moreover, the commands applied to the set of thrusters including 1–8, in the present experiment, are all shown in Figs. 5, 6 respectively.

In the second experiment, the tracking of the three-axis angular velocities of the spacecraft are now presented in Fig. 7. In this case, the desired commands are taken as 0.1, 0.3, 0.2 °/s to be applied to the approach.

Moreover, the commands applied to the set of thrusters are shown in Figs. 8, 9 respectively.

In the third experiment, the tracking of the three-axis angular velocities of the spacecraft are now presented. In the same way, Fig. 10 illustrates the investigated results, since the desired commands are taken as 0, 0, 0.3 °/s to be applied to the approach.

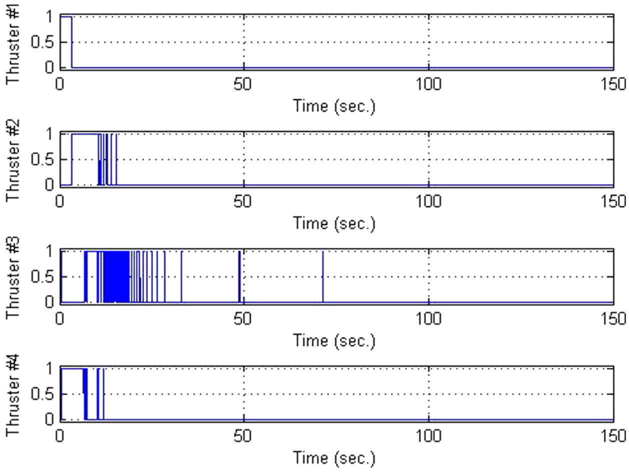

Fig. 5 The thruster's commands—1:4 in the 1st experiment

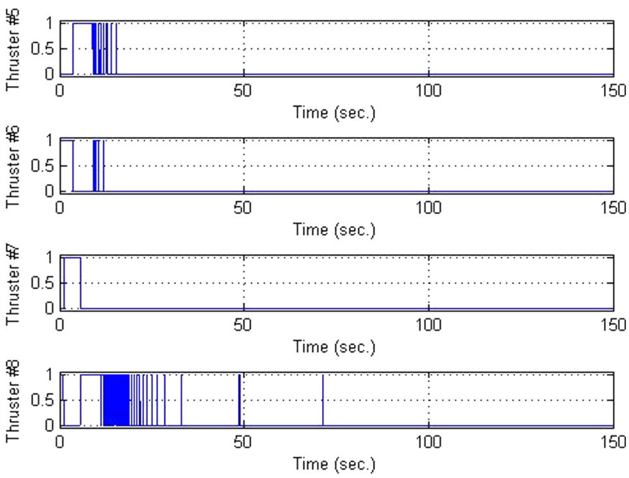

Fig. 6 The thruster's commands—5:8 in the 1st experiment

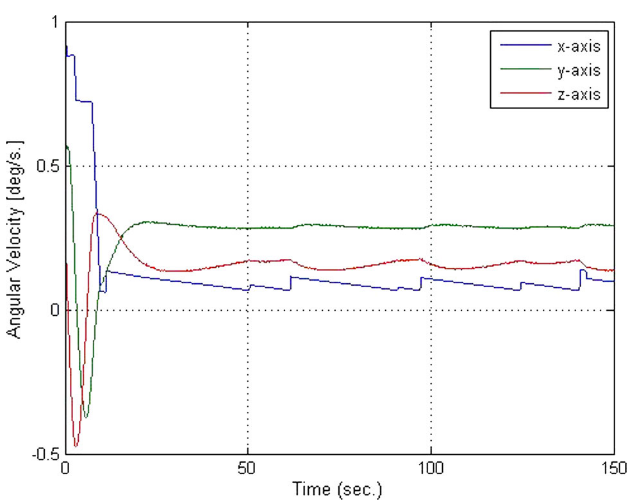

Fig. 7 The tracking of three-axis angular velocities of the system in the 2nd experiment

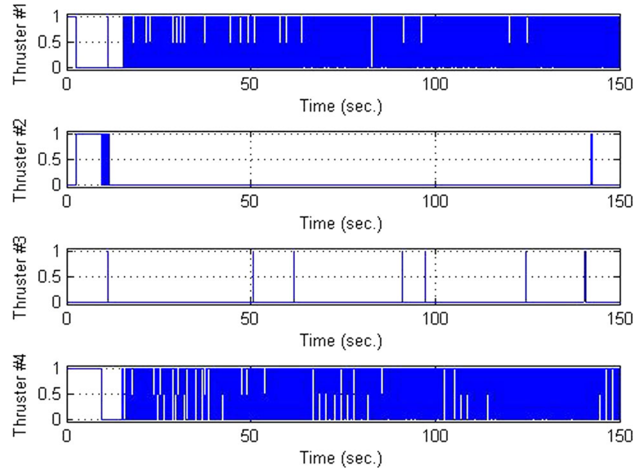

Fig. 8 The thruster's commands—1:4 in the 2nd experiment

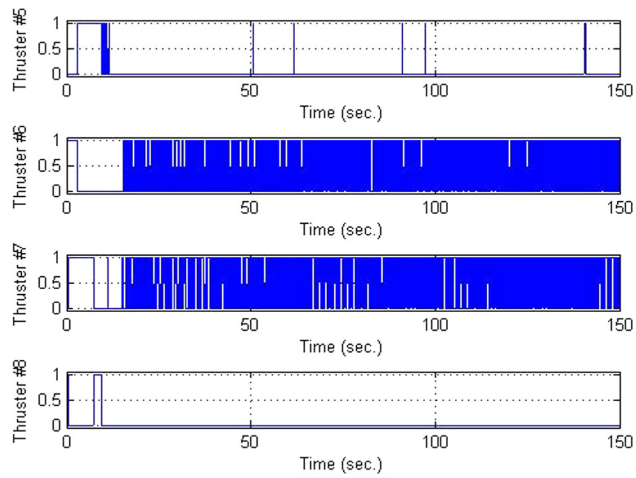

Fig. 9 The thruster's commands—5:8 in the 2nd experiment

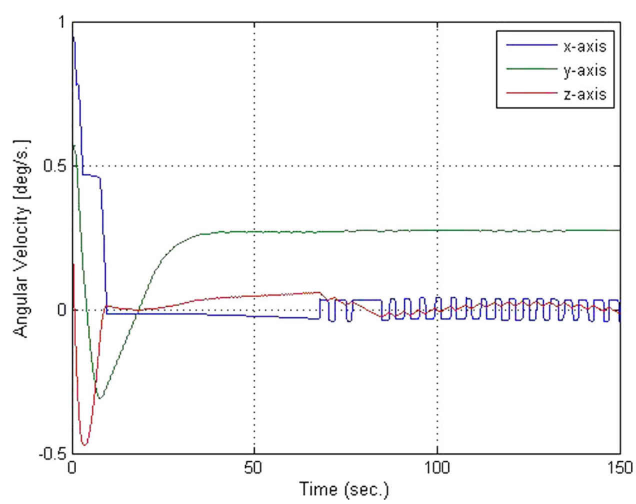

Fig. 10 The tracking of three-axis angular velocities of the system in the 3rd experiment

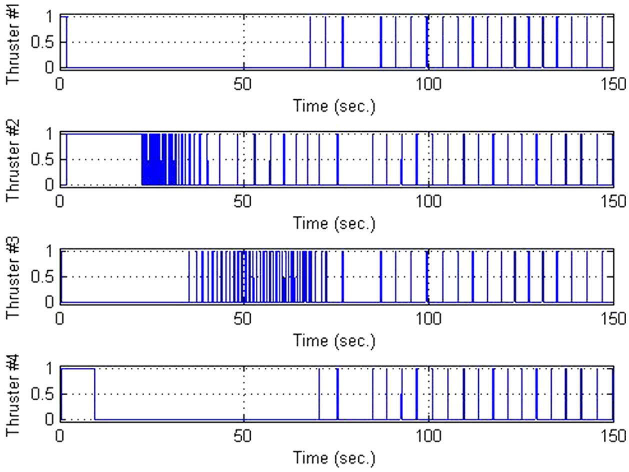

Fig. 11 The thruster's commands—1:4 in the 3rd experiment

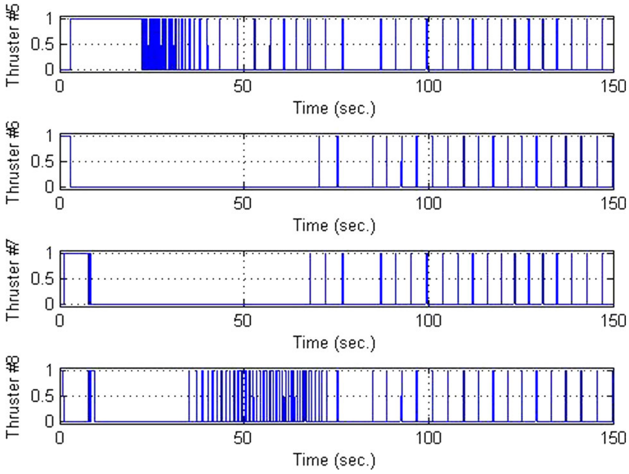

Fig. 12 The thruster's commands—5:8 in the 3rd experiment

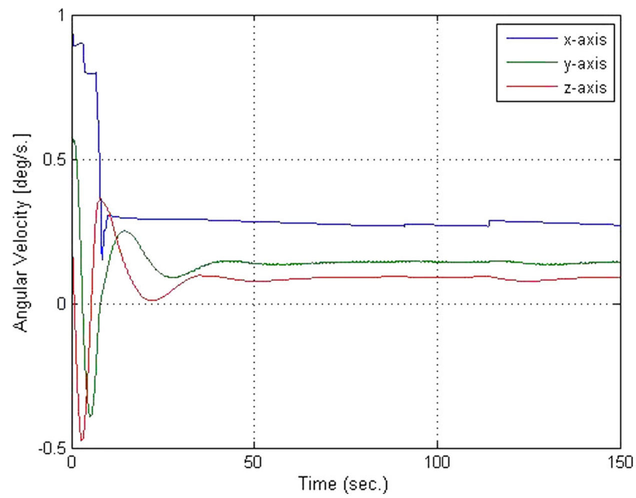

Fig. 13 The tracking of three-axis angular velocities of the system in the 4th experiment

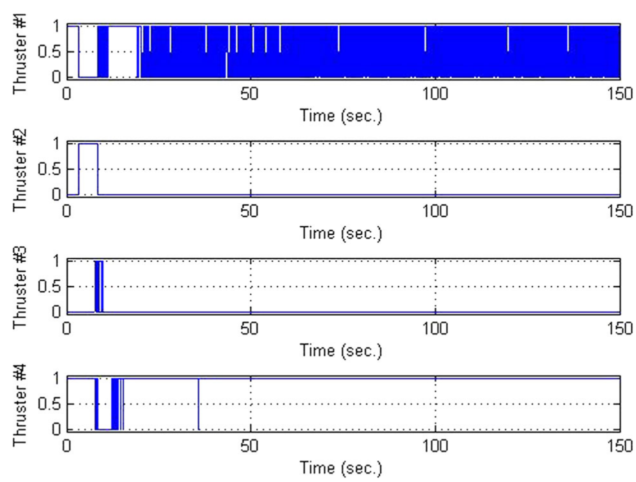

Fig. 14 The thruster's commands—1:4 in the 4th experiment

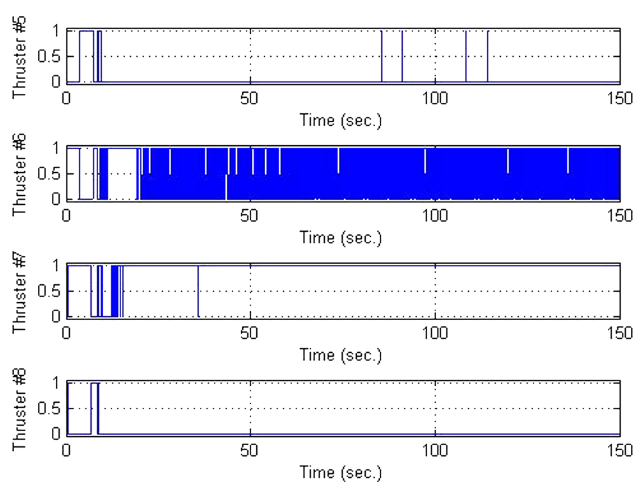

Fig. 15 The thruster's commands—5:8 in the 4th experiment

Moreover, the commands applied to the set of thrusters are given in Figs. 11, 12 respectively.

In the last experiment, the tracking of the three-axis angular velocities of the spacecraft are finally presented in Fig. 13. In the same way, the desired commands are taken as 0.3, 0.2, 0.15 °/s that are applied to the approach.

Moreover, the commands applied to the set of thrusters are given in Figs. 14, 15 respectively.

Also, in order to verify the investigated results, two references, researched in the recent years, are now considered to be compared as the benchmarks. With this purpose, the Lin approach is to realize a two-part method for detumbling a rigid spacecraft through a set of three-axis magnetic torque. Hereinafter, the Ovchinnikova approach is to realize the angular motion of a satellite that is equipped with the active magnetic attitude control system.

Table 4 The proposed approach performance verification w.r.t. the corresponding benchmarks

	The approach titles	Maximum three-axis angular velocities errors in steady state (°/s)	Trajectory convergence time (s)
1	The Lin approach [1]	<0.08	>100
2	The Ovchinnikova approach [2]	<0.02	>100
3	The proposed approach	<0.05	< 30

These research strategies are somehow comparable with respect to the proposed approach. There are the following criteria to be analyzed in Table 4 including (1) the maximum three-axis angular velocities errors in steady state and (2) the trajectory convergence time, which are all important to evaluate the approach performances with respect to the corresponding benchmarks.

As a deduction matter, the results indicate that the proposed approach can be considered regarding the mentioned items, where the Ovchinnikova approach is well behaved regarding the item (1) with respect to both the present considerable approaches. Finally, the proposed approach is somehow well behaved regarding the item (1) with respect to the Lin approach and also the item (2) with respect to both approaches, as well.

5 Conclusion

The realization of the detumbling mode control approach in the area of spacecraft is important to guarantee the system stability. It aims the spacecraft to adjust the three-axis angular velocities in the process of the separation of the spacecraft. It means that the spacecraft is not truly able to cover a specified mission if the angular velocities in the three axes cannot be dealt with, appropriately. With a focus on state-of-the-art in this area, the present study considers the problem of detumbling mode control by proposing the new control approach in association with the system modelling. It is organized based upon the closed loop system including the proportional derivative control, the PWPF modulator, the control allocation and finally the spacecraft dynamics. It is shown that the responsibility of the present proportional derivative control is to deal with the angular velocities of the spacecraft in the three axes to guarantee the tracking performance, in a short period of time, accurately. The PWPF modulator is realized in association with the control allocation to produce the required control efforts, at each instant of time, to satisfy the spacecraft performance. Due to the fact that the number of required thrusters in the present research is more than the three-axis control torques, the CA scheme has to be employed to deal with the thrusters. In fact, the signals, produced through the control allocation, are applied to a number of employed on–off thrusters. The idea of the proposed approach is completed by employing the three-axis desired referenced generator module, the data conversion module, the inverse data conversion module and finally the uncertainties and disturbances generator. Finally, the proposed approach performance is considered through four scenarios of the experiments. Analysis of the simulation results indicate that the investigated outcomes are able to deal with the three-axis angular velocities. The proposed approach performance is considered once again by comparing its outcomes with a number of potential benchmarks.

Acknowledgments The corresponding author would like to express all the best and the warmest regards to the respected Editor of 'International Journal of Dynamics and Control (IJDY)', Springer Publisher, as well as the whole of respected potential reviewers, for suggesting their impressive, constructive and technical comments on the present investigation. Afterwards, Dr. Mazinan is highly grateful to the Islamic Azad University (IAU), South Tehran Brach, Tehran, Iran in support of the present research, which is carried out under contract with the Research Department of the IAU, South Tehran Brach. And also he appreciates Mrs. Maryam Aghaei Sarchali, Miss Mohadeseh Mazinan and finally Mr. Mohammad Mazinan for their sufficient supports in the process of paper investigation and organization.

Conflict of interest The authors declare that there is no conflict of interest.

References

1. Lin Y-Y, Wang C-T (2014) Detumbling of a rigid spacecraft via torque wheel assisted gyroscopic motion. Acta Astronaut 93:1–12
2. Ovchinnikova MY, Roldugin DS, Penkov VI (2012) Asymptotic study of a complete magnetic attitude control cycle providing a single-axis orientation. Acta Astronaut 77:48–60
3. Santana AC, Martins-Filho LS, Arantes G Jr (2008) Attitude stabilization of the PMM satellite using a LQG-based control strategy. TEMA Trends Appl Comput Math 9(2):321–330. doi:10.5540/tema.2008.09.02.0321
4. Zhang W, Zeng J, Li Y (2013) A review of vehicle system dynamics in the development of high-speed trains in China. Int J Dyn Control 1(1):81–97
5. Farid Y, Moghaddam TV (2014) Generalized projective synchronization of chaotic satellites problem using linear matrix inequality. Int J Dyn Control 2(4):577–586
6. Sabatini M, Palmerini GB, Leonangeli N, Gasbarri P (2014) Analysis and experiments for delay compensation in attitude control of flexible spacecraft. Acta Astronaut 104(1):276–292
7. Sidi MJ (1997) Spacecraft dynamics and control, a practical engineering approach, vol 7. Cambridge University Press, Cambridge

8. Zipfel PH (2000) Modeling and simulation of aerospace vehicle dynamics. AIAA, USA
9. Zheng Z, Song S (2014) Autonomous attitude coordinated control for spacecraft formation with input constraint, model uncertainties, and external disturbances. Chin J Aeronaut 27(3):602–612
10. Yang H, You X, Xia Y, Liu Z (2014) Nonlinear attitude tracking control for spacecraft formation with multiple delays. Adv Space Res 54(4):759–769
11. Huo X, Qinglei H, Xiao B (2014) Finite-time fault tolerant attitude stabilization control for rigid spacecraft. ISA Trans 53(2):241–250
12. Du H, Li S (2014) Attitude synchronization control for a group of flexible spacecraft. Automatica 50(2):646–651
13. Song Z, Li H, Sun K (2014) Finite-time control for nonlinear spacecraft attitude based on terminal sliding mode technique. ISA Trans 53(1):117–124
14. Lu K, Xia Y (2013) Adaptive attitude tracking control for rigid spacecraft with finite-time convergence. Automatica 49(12):3591–3599
15. Yang Y (2012) Spacecraft attitude determination and control: quaternion based method. Annu Rev Control 36(2):198–219
16. Zou A-M, Kumar KD (2011) Adaptive fuzzy fault-tolerant attitude control of spacecraft. Control Eng Pract 19(1):10–21
17. Qinglei H, Li B, Zhang Y (2013) Robust attitude control design for spacecraft under assigned velocity and control constraints. ISA Trans 52(4):480–493
18. Cai H, Huang J (2014) The leader-following attitude control of multiple rigid spacecraft systems. Automatica 50(4):1109–1115
19. Kuo Y-L, Wu T-L (2012) Open-loop and closed-loop attitude dynamics and controls of miniature spacecraft using pseudowheels. Comput Math Appl 64(5):1282–1290
20. Zhang X, Liu X, Zhu Q (2014) Attitude control of rigid spacecraft with disturbance generated by time varying exosystems. Commun Nonlinear Sci Numer Simul 19(7):2423–2434
21. Erdong J, Xiaolei J, Zhaowei S (2008) Robust decentralized attitude coordination control of spacecraft formation. Syst Control Lett 57(7):567–577
22. Bustan D, Pariz N, Sani SKH (2014) Robust fault-tolerant tracking control design for spacecraft under control input saturation. ISA Trans 53(4):1073–1080
23. Lu K, Xia Y, Fu M (2013) Controller design for rigid spacecraft attitude tracking with actuator saturation. Inf Sci 220(20):343–366
24. Pukdeboon C, Zinober ASI (2012) Control Lyapunov function optimal sliding mode controllers for attitude tracking of spacecraft. J Frankl Inst 349(2):456–475
25. Yongqiang J, Xiangdong L, Wei Q, Chaozhen H (2008) Time-varying sliding mode controls in rigid spacecraft attitude tracking. Chin J Aeronaut 21(4):352–360
26. Wu J, Liu K, Han D (2013) Adaptive sliding mode control for six-DOF relative motion of spacecraft with input constraint. Acta Astronaut 87:64–76
27. Jiang Y, Hu Q, Ma G (2010) Adaptive backstepping fault-tolerant control for flexible spacecraft with unknown bounded disturbances and actuator failures. ISA Trans 49(1):57–69
28. Butyrin SA, Makarov VP, Mukumov RR, Somov Y, Vassilye SN (1997) An expert system for design of spacecraft attitude control systems. Artif Intell Eng 11(1):49–59
29. Hu Q, Zhang J (2014) Relative position finite-time coordinated tracking control of spacecraft formation without velocity measurements. ISA Trans. Corrected Proof, Available online 27 August (in press)
30. Krovel T (2005) Optimal tuning of PWPF modulator for attitude control. Master’s thesis, Norwegian University of Science and Technology, Trondheim, Norway
31. Johansen TA, Fossen TI (2013) Control allocation—a survey. Automatica 49(5):1087–1103
32. Zaccarian L (2009) Dynamic allocation for input redundant control systems. Automatica 45(6):1431–1438
33. Servidia PA (2010) Control allocation for gimballed/fixed thrusters. Acta Astronaut 66(3–4):587–594